Target Structural Reliability Analysis for Tsunami Hydrodynamic Loads of the ASCE 7 Standard

Gary Chock, Dist.M.ASCE[1]; Guangren Yu, M.ASCE[2]; Hong Kie Thio[3]; Patrick J. Lynett, M.ASCE[4]

Abstract: Many coastal areas in the United States are subject to tsunami hazard. The public safety risk has been partially mitigated through warning and preparedness of evacuation, but community disaster resilience requires that critical and essential facilities provide structural resistance to collapse. Furthermore, there are coastal communities in the states of Alaska, Washington, Oregon, California, and Hawaii where there is insufficient time for evacuation. The Tsunami Loads and Effects Subcommittee of the ASCE/Structural Engineering Institute (ASCE/SEI) 7 Standards Committee has developed a new Chapter 6, titled "Tsunami Loads and Effects," for the 2016 edition of the ASCE 7 standard Minimum Design Loads for Buildings and Other Structures (*Minimum design loads for buildings and other structures*). The new ASCE 7 provisions for tsunami loads and effects implements a unified set of analysis and design methodologies that are consistent with probabilistic hazard analysis, tsunami physics, and reliability analysis. The purpose of this paper is to provide analysis of the structural reliability basis for tsunami-resilient design of critical and essential facilities, taller building structures, and tsunami vertical evacuation refuge structures. Probabilistic limit-state reliabilities are computed for representative structural components carrying gravity and tsunami loads, utilizing statistical information on the key hydrodynamic loading parameters and resistance models with specified tsunami load combination factors. Through a parametric analysis performed using Monte Carlo simulation, it is shown that anticipated reliabilities for tsunami hydrodynamic loads meet the general intent of the ASCE 7 standard as stated in its Chapter 1 commentary. Importance factors consistent with the target reliabilities for extraordinary loads (such as seismic events) are determined for tsunami loads. **DOI: 10.1061/(ASCE)ST.1943-541X.0001499.**

Author keywords: Tsunami; Safety; Reliability; ASCE 7 standard; Safety and reliability.

Introduction

Tsunamis are infrequent events but can be extremely destructive. A tsunami is a series of great waves primarily caused by a major subduction zone earthquake with large-scale displacement of the sea floor or by initiation of submarine landslides. Many coastal areas in the United States are subject to tsunami hazard. The public safety risk has been partially mitigated through warning and preparedness of evacuation, but community disaster resilience requires that critical and essential facilities provide structural resistance to collapse. Furthermore, there are coastal communities in the states of Alaska, Washington, Oregon, California, and Hawaii where there is insufficient time for evacuation. With these circumstances, the availability of taller buildings that are tsunami resistant is a direct benefit to public safety. The recent catastrophic tsunamis in the Indian Ocean (2004), Samoa (2009), Chile (2010), and Japan (2011) indicate that an explicit structural design procedure for risk mitigation of tsunami damage to major structures is much needed. Multistory buildings, which are necessary for tsunami safety where evacuation cannot be completely assured, can be economically designed for life safety or better performance for large tsunamis with local strengthening of relatively few components.

The 2016 edition of the ASCE 7 standard, *Minimum design loads for buildings and other structures* will introduce a new Chapter 6, titled "Tsunami Loads and Effects" (ASCE 2016). Tsunami risk categories are based on the risk categories defined in Section 1.5 of ASCE 7, with some modifications for specific types of structures allowed per ASCE 7-16 Section 6.4 for tsunami conditions in the local community (the local government would need to identify their critical facilities versus those facilities that are not uniquely required for posttsunami functionality). Tsunami Risk Category III and Tsunami Risk Category IV buildings and other structures located in the tsunami-prone states of Alaska, Washington, Oregon, California, and Hawaii shall be designed to resist the tsunami loads and effects determined for a maximum considered tsunami. Recent United States and international research and validation by documented case studies of tsunami flows and their effects on structures were utilized in developing this chapter and commentary, along with the development of new probabilistic tsunami design zone maps (Chock 2016).

Tsunami Vertical Evacuation Refuge Structures

In ASCE 7-16, a tsunami vertical evacuation refuge structure is a special type of Risk Category IV structure with additional design requirements. This structure serves as a designated point of refuge to which a portion of a community's population can evacuate when higher ground is not reachable in time before tsunami arrival. A particularly important consideration is the elevation and height of the refuge, since it must provide very high reliability of structural life safety for the occupants within a portion of the refuge that is not

[1]Structural Engineering Institute Fellow, Chair, ASCE 7 Tsunami Loads and Effects Subcommittee; President, Martin & Chock, Inc., 1132 Bishop St., Suite 1550, Honolulu, HI 96813 (corresponding author). E-mail: gchock@martinchock.com

[2]Structural Engineer, Martin & Chock, Inc., 1132 Bishop St., Suite 1550, Honolulu, HI 96813. E-mail: gyu@martinchock.com

[3]Vice President, Principal Seismologist, AECOM, 915 Wilshire Blvd., 7th Floor, Los Angeles, CA 90017. E-mail: hong.kie.thio@aecom.com

[4]Professor, Dept. of Civil and Environmental Engineering, Univ. of Southern California, KAP 224D, Los Angeles, CA 90089. E-mail: plynett@usc.edu

Note. This manuscript was submitted on May 12, 2015; approved on December 17, 2015; published online on May 24, 2016. Discussion period open until October 24, 2016; separate discussions must be submitted for individual papers. This paper is part of the ***Journal of Structural Engineering***, © ASCE, ISSN 0733-9445.

inundated. Therefore, additional conservatism is necessary in the estimation of inundation height for the design of these special occupancy structures. The minimum elevation for a tsunami vertical evacuation refuge structure is the maximum considered tsunami runup elevation anticipated at the site, increased by 30%. A site-specific tsunami inundation time history analysis is required for a tsunami vertical evacuation refuge, as well as an importance factor of 1.25.

Tsunami Hazard Analysis

The enduring lesson of recent catastrophic tsunamis is that historical records alone do not provide a sufficient measure of the potential heights of future tsunamis. Engineering design must consider the occurrence of events greater than scenarios in the historical record, based on the underlying seismicity of subduction zones. To achieve a consistent structural performance for community resilience, a probabilistic tsunami inundation geodatabase for design is digitally available with the ASCE tsunami design provisions. The tsunami design zone is the area vulnerable to being inundated by the maximum considered tsunami (MCT), which is taken as having a 2% probability of being exceeded in a 50-year period or a 2,475-year mean recurrence interval. A probabilistic tsunami hazard analysis (PTHA), which is similar to probabilistic seismic hazard analysis (PSHA), was performed to produce hazard-consistent offshore tsunami amplitude waveform data and tsunami design zone inundation and runup map data. An early example of the PTHA procedure was initially performed for California (Thio et al. 2010), which was subsequently refined in accordance with a peer review study sponsored by the National Tsunami Hazard Mitigation Program (California Geological Survey 2015).

Tsunami loads and effects are based on the MCT that is characterized by the inundation depth and flow velocities during the stages of inflow and outflow at the site. There are two procedures for determining the MCT inundation depth and velocities at a site: (1) the energy grade line analysis (EGLA); and (2) a site-specific inundation analysis (Chock 2015). The EGLA is fundamentally a hydraulic analysis along a topographic transect from the shore line to the runup point which takes the runup elevation and inundation limit indicated on the tsunami design zone map as the given solution point. It generally produces values of design flow parameters that are conservatively greater than numerical modeling of the same transect, and so it is always performed as the minimum baseline analysis of the site. (Carden et al. 2015). Site-specific inundation analysis utilizes the offshore tsunami amplitude, the effective wave period that is considered a conserved property, and other specified waveform shape parameters as the input; it is a two-dimensional (2D) numerical simulation based on a higher-resolution digital elevation model of nearshore bathymetry and onshore topography. The site-specific inundation analysis is required to be performed for Tsunami Risk Category IV structures unless the energy grade line analysis shows the inundation depth to be less than 3.66 m (12 ft) at the structure. The design of tsunami vertical refuge structures always utilizes a site-specific inundation analysis.

For this reliability analysis study, representative vertical-load-carrying components of prototypical buildings have been evaluated for tsunami load effects at three prototypically located sites at each of two regions (Huntington Beach and Crescent City, California). The three sites at each region are located at the shoreline, and one-quarter and one-half of the inundation distance inland (where $x = 0.0X_R$, $x = 0.25X_R$, and $x = 0.5X_R$; Fig. 1 for $x = 0.0X_R$, $0.25X_R$, and $0.5X_R$). Probabilistic tsunami hazard analysis was performed to obtain prototypical offshore tsunami amplitude hazard curves and the associated inland tsunami inundation depth hazard curves for the six sites. As an example, Fig. 2 shows the offshore and the two inland inundation depth hazard curves at Crescent City, California.

Basic Limit-State Equation and Tsunami Design Parameters

The following load combinations with tsunami forces as the primary load effect are specified in ASCE 7-16 by Eqs. (1) and (2):

$$\phi R_n = 1.2D_n + 1.0F_{\mathrm{TSUn}} + 0.5L_n \tag{1}$$

$$\phi R_n = 0.9D_n + 1.0F_{\mathrm{TSUn}} \tag{2}$$

in which ϕ = resistance factor; R_n = nominal strength; D_n = nominal dead load; L_n = nominal live load; and F_{TSUn} = nominal tsunami effect. The nominal subscript notation refers to the specified loads and resistances, per the convention of engineering reliability analysis.

Lateral hydrodynamic tsunami forces are generally much greater than hydrostatic lateral and buoyant vertical tsunami forces. When considering the out-of-plane strength capacity of a reinforced concrete wall or a steel or concrete column element subject to tsunami hydrodynamic forces, the vertical dead and live loads are perpendicular to the lateral tsunami hydrodynamic force, so the vertical loads do not contribute to the direct action but are also not counteracting loads to the tsunami hydrodynamic forces. That is, the primary hydrodynamic load is lateral pressure on vertical elements, so the dead load and live load do not directly counteract

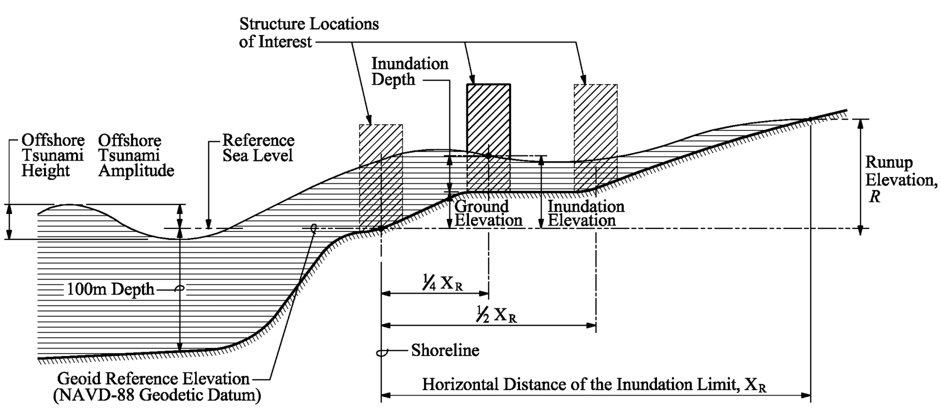

Fig. 1. Locations of three prototypically located sites along the transect

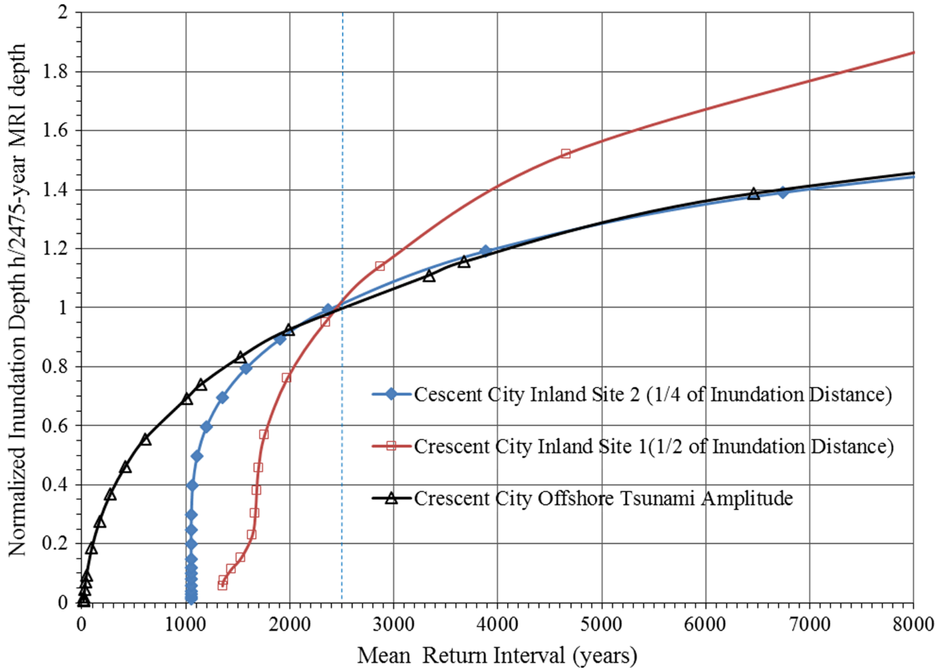

Fig. 2. Normalized Crescent City inland site inundation hazard curve and offshore hazard curve (inundation depth hazard curve is normalized to the depth for the MCT)

the tsunami load for those elements [in contrast to the reliability analysis of wind uplift pressure on roof structural components, for example, in Ellingwood et al. (1980)]. However, the design for vertical dead and live loads results in resistive capacity, R_n, in the vertical (beam–column) member that has biaxial axial load–moment (P–M) capacity to resist the lateral pressures, rather than acting as a purely flexural beam member.

Tsunami-resistant structures will predominately be in the height regime of four or more stories, and the beam–column resistance should also reflect the column design capacity that includes dead and live load, $1.2D + 1.6L$ (ASCE 2016). There is a beneficial effect in flexural capacity of the vertical beam–column under tsunami lateral load component due to the $0.5L$ axial loading in the load combination given in Eq. (1). Based on prototypical tsunami designs compared to a purely flexural beam (Robertson 2016), the capacity bias for the beam–column designed for vertical load is estimated to be lognormal with about a mean of 1.15 and a sigma of 0.2, i.e., a coefficient of variation (COV) of 0.17. Assuming λ_n is the capacity factor of a flexural member, Eqs. (1) and (2) would be revised to account for beam–column behavior as follows in Eq. (3):

$$\lambda_n \phi R_n = 1.0 F_{\mathrm{TSUn}} \tag{3}$$

For beam–column bending, the general limit-state function $G(X) = R - S$, i.e., the expression for Resistance–Load can be formulated in Eq. (4) as

$$G(X) = G(R, \lambda, F_{\mathrm{TSU}}) = \lambda R - F_{\mathrm{TSU}} \tag{4}$$

in which λ = capacity bias of the beam-column considering effects of axial loading of dead and live loads. Using Eq. (3) to normalize the expression, the limit-state function becomes Eq. (5):

$$\frac{1}{\lambda_n \phi R_n} G(X) = \frac{1}{\lambda_n \phi R_n} G(R, \lambda, F_{\mathrm{TSU}}) = \frac{\lambda}{\lambda_n} \frac{R}{\phi R_n} - \frac{F_{\mathrm{TSU}}}{F_{\mathrm{TSUn}}} \tag{5}$$

Assuming λ/λ_n and R/R_n are statistically independent relationships with their COVs being 0.17 and 0.11 or 0.13, respectively, the net COV for the capacity of a beam–column would have values of 0.20 or 0.22 for reinforced concrete and structural steel. This value is slightly higher than the 0.17 suggested by Ellingwood (1977), meaning that a greater amount of uncertainty is considered in this analysis. Considering tension-governing failure is typically induced by tsunami lateral loading, the COV of 0.21 was the net uncertainty that results from the random variables λ/λ_n and R/R_n for the capacity of the beam–columns subject to tsunami loading as the principal action.

The lateral hydrodynamic load given by Eq. (6) is assumed to govern when a vertical beam–column is subject to tsunami loading

$$F_{\mathrm{TSU}} = \frac{1}{2} \rho_s C_d b (h_e u^2) I_{\mathrm{tsu}} \tag{6}$$

in which ρ_s = minimum fluid mass density; C_d = drag coefficient for the building component; b = width perpendicular to the flow; h_e = inundation depth; u = flow velocity; and I_{tsu} = tsunami importance factor.

The second term on the right side of the limit-state function [Eq. (5)] is then expanded to Eqs. (7) and (8):

$$\frac{F_{\mathrm{TSU}}}{F_{\mathrm{TSUn}}} = \frac{\frac{1}{2} \rho_s C_d b (h_e u^2)}{\frac{1}{2} \rho_{sn} C_{dn} b_n (h_e u^2)_n I_{\mathrm{tsu}}} \tag{7}$$

$$\frac{F_{\mathrm{TSU}}}{F_{\mathrm{TSUn}}} = \frac{\rho_s}{\rho_{sn}} \frac{C_d}{C_{dn}} \frac{b}{b_n} \frac{(h_e u^2)}{(h_e u^2)_n} \frac{1.0}{I_{\mathrm{tsu}}} \tag{8}$$

in which ρ_{sn}, C_{dn}, b_n, and $(h_e u^2)_n$ = nominal design values. The term $(h_e u^2)_n$ refers to the momentum flux calculated in accordance with the EGLA. Introducing $(h_e u)_o$ as the momentum flux obtained by a detailed numerical model for site-specific inundation analysis, Eq. (8) then can be expressed in the form of Eq. (9):

$$\frac{F_{\mathrm{TSU}}}{F_{\mathrm{TSUn}}} = \frac{\rho_s}{\rho_{sn}} \frac{C_d}{C_{dn}} \frac{b}{b_n} \frac{(h_e u^2)_o}{(h_e u^2)_n} \frac{(h_e u^2)}{(h_e u^2)_o} \frac{1.0}{I_{\mathrm{tsu}}} \tag{9}$$

The depth-averaged flow velocity is considered to be a function of inundation depth, as expressed by the Froude number for tsunami flow [the nondimensionalized flow velocity $u/\sqrt{(gh)}$] that is prescribed to decay gradually based on distance from the shoreline along the transect in accordance with the EGLA (Chock 2015). Eq. (9) is then parametrically simplified to an expression relating to the inundation depth as Eq. (10):

$$\frac{F_{\text{TSU}}}{F_{\text{TSUn}}} = \frac{\rho_s}{\rho_{sn}} \frac{C_d}{C_{dn}} \frac{b}{b_n} \psi \left(\frac{h_e}{h_{eo}}\right)^2 \frac{1.0}{I_{\text{tsu}}} \tag{10}$$

In Eq. (10), $\psi = (h_e u^2)_0/(h_e u^2)_n$; and h_{eo} = inundation depth with a 2,475-year return period. Including the effect of aleatory uncertainties, h_e is εh where h is the inundation depth without considering the effect of aleatory uncertainties and ε accounts for the net aleatory uncertainties in estimated inundation depth associated with the modeling of seismic sources and inundation numerical modeling.

Since the terms $\lambda_n \phi R_n$ at the left side of Eq. (5) are not random and always greater than 0, the fundamental limit-state equation can thus be further developed to Eq. (11):

$$G(X) = \frac{\lambda}{\lambda_n} \frac{R}{\phi R_n} - \frac{\rho_s}{\rho_{sn}} \frac{C_d}{C_{dn}} \frac{b}{b_n} \psi \varepsilon^2 \left(\frac{h}{h_{eo}}\right)^2 \frac{1.0}{I_{\text{tsu}}} \tag{11}$$

in which $G(X) = G(R, \lambda, F_{\text{TSU}}) = G(R/R_n, \lambda/\lambda_n, \rho_s/\rho_{sn}, C_d/C_{dn}, b/b_n, \psi, \varepsilon, h_e/h_{en})$

Reliability Analysis Parameters for Tsunamis

For drag coefficients, C_d/C_{dn} is assumed to be a constant value of 1.0. The drag coefficients are form-dependent values from the recognized literature; as an example of lack of significant bias, the true value of C_d drag coefficient for a cylinder is 1.17 and the specified value is 1.2.

For fluid density, ρ_s/ρ_{sn} is assumed to vary with a normal distribution with mean of 1.0 and a COV of 0.03. The mean of the specified fluid density factor, k_s is considered to be 1.1 accounting for suspended material and embedded smaller debris carried in the flow so that ρ_s is defined by $k_s \rho_{sw}$ (in which ρ_{sw} is the seawater mass density) with the expectation that this variable could vary between 1.05 and 1.15 (yielding a COV for k_s of 0.030) with 1.10 as the mean effective fluid mass density representing a debris flood rather than pure seawater (a debris flood is laden with sediment and suspended debris, but still behaves essentially as a fluid rather than a flow with plastic viscosity).

Regarding width, b/b_n is assumed to be uniformly distributed with the range of 0.4/0.7 and 0.6/0.7 (i.e., [0.571, 0.857] with a mean of 0.71). To account for assorted debris accumulation, ASCE 7 does not allow the forces to be computed on the bare structure without cladding, interior walls and fixtures, or contents. For buildings initially cladded, the designer can conservatively assume only 30% of this becomes open to allow unimpeded flow. Actual accumulation is estimated from field case studies (Carden et al. 2015) to be in the range of creating a 40 to 60% closure ratio, rather than the prescribed 70% as used for design, so there is some conservative bias in the design provisions to prevent underestimation of loading. The prescriptive minimum closure ratio of 70% of overall building width is biased upward by about 0.7/0.5, assuming a uniform distribution with the COV of 0.115. This prescribed minimum ratio is applied to the vertical projected tributary area of the exterior component or structure being designed. For interior column and wall components, ASCE 7 does not have this restriction, and hydrodynamic forces are computed on the bare structural form of the interior components. The likelihood of debris accumulation on interior columns is much less than on exterior columns along the building perimeter. Therefore, the reliabilities are calculated with this biased closure ratio design parameter for exterior columns, and without this closure ratio parameter for the case of interior columns.

For inundation depth, h_e/h_{en} is sampled from the cumulative distribution function (CDF) of 50-year service life maximum inundation depth as illustrated in Fig. 3, which shows the details of the upper tail of the CDF derived from the hazard curve obtained through probabilistic tsunami hazard analysis (PTHA). At inland sites such as this example case of $x = 0.025x_R$ at Crescent City, the higher frequency, lower-runup tsunami events do not reach the site, leading to a statistical clustering of data until more significant and rarer events overwash the site. In addition, h_e is the inundation depth without considering aleatory uncertainties, and h_{en} is the specified value (i.e., inundation depth with a 2,475-year return period including the effect of aleatory uncertainties). Above a 5,000-year MRI, tsunami inundation depth is considered to have reached a plateau value. The reliability analysis given here is based on inland hazard curves since the subject application is primarily buildings.

For aleatory uncertainty, ε accounts for the net aleatory uncertainties in estimated inundation depth associated with the modeling of seismic sources and numerical modeling of inundation based on field case studies, and this is modeled with a lognormal distribution ($\lambda = 0$ and $\zeta = 0.30$ or mean $= 1.06$ and COV $= 0.283$) when high-resolution digital elevation models are used. Aleatory variability is taken into account at several stages in the probabilistic analysis: in the source by considering magnitude distribution functions and multiple distributed slip models, and in the tsunami propagation term by applying a distribution function to the offshore tsunami amplitudes. It is the latter term that is of concern in this analysis since it is dominated by limits in present modeling accuracy. The main components of aleatory uncertainty are approximations in tsunami inundation modeling algorithms and details in the seismic rupture process that cannot be resolved.

Aleatory variability and epistemic uncertainty are generally used in discussions of probabilistic seismic hazard analysis (PSHA). In PSHA, this term is considered as the inherent part of the empirically obtained ground motion prediction equations. In PTHA, the aleatory uncertainty is measured explicitly through ground-truthing statistics. Estimates of the aleatory uncertainty were obtained by comparing tsunami data (tide-gauge data, maximum water heights at the shore, and runup elevations) and model results for well-constrained (in terms of slip model) tsunamigenic sources, such as the 2011 Tohoku earthquake. Since the analysis is divided into offshore tsunami amplitude and onshore inundation results, and since the propagation characteristics are very different between the two regimes, sigma terms for each component were estimated in the determination of the net uncertainty given in the earlier discussion. The aleatory uncertainty for the seismic source modeling is lognormal with a sigma of 0.25, and the aleatory uncertainty for the inundation modeling is lognormal with a sigma of 0.15, for a total sigma of 0.29, or about 0.30 as used here with a mean of 1.067, yielding a COV of 0.283. Also, these aleatory variability estimates are strictly applicable only to model grid resolutions that are similar to the resolutions used in the lognormal distribution sigma analysis for the ASCE 7 tsunami provisions; that is, the statistical estimate of aleatory variability in this application is within the context of the PTHA and inundation model used and what is observed in actual event data.

Epistemic uncertainty in prescriptive analysis of flow: ψ is a variable to account for the epistemic uncertainty in the nominal solution (i.e., imprecisions in the code-specified energy grade line

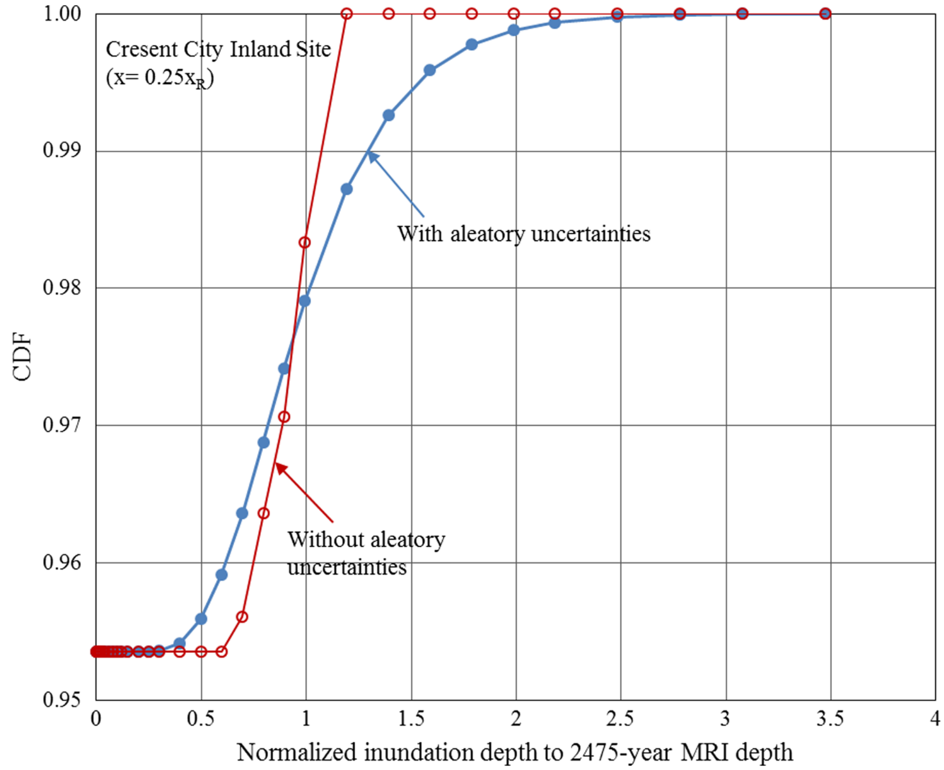

Fig. 3. Cumulative distribution function of normalized inundation depth for Crescent City Site 2 at $x = 0.25x_R$

analysis) versus numerical model. It is sampled from the normalized momentum flux hazard curve (Fig. 4) in accordance with the bias and COV statistics of the EGLA versus numerical simulation model (Lynett and Liu 2011). The next section describes how this variable is derived for the normalized momentum flux hazard curve. The EGLA is deemed sufficient for Tsunami Risk Category II and III structures; for Tsunami Risk Category IV structures and tsunami vertical evacuation refuge structures, a site-specific inundation analysis is necessary.

For structural resistance, R/R_n is assumed to be normally distributed. For a concrete flexural member, the mean is 1.05 and the COV is 0.11. For compact steel beams or columns, the mean is 1.07 and the COV is 0.13 (Ellingwood et al. 1980).

Statistical Assessment of the Energy Grade Line Analysis to Derive ψ

A robust comparison of the EGLA with a detailed inundation model was performed to assess the ability of the EGLA to provide a conservative result for a wide range of possible onshore topographic profiles and wave conditions. The general approach employed was to run a number of simulations using a Boussinesq-type model (Lynett and Liu 2011) and compare the inundation properties of the Boussinesq output with the EGLA. Nonlinear Boussinesq equation-based algorithms have been used for long-wave modeling, wave diffraction and nonlinear dispersive waves, wave breaking, and other unsteady shallow-water flow. Specifically, the procedure for a single comparison case was performed as follows:

1. Generate a beach profile; the profile starts at an offshore depth of 100 m and extends onshore to an elevation of 50 m.
2. Generate an incident wave condition; the condition consists of an initial trough or crest elevation, a following crest or trough elevation, and a characteristic period of the waveform.
3. Run a Boussinesq simulation with these profile and wave inputs; the resolution used here is 10 m across the length of the entire profile with the simulations using a typical Manning's n friction factor of 0.025 at all grid points (both offshore and onshore); this value is per ASCE 7 Chapter 6 specifications.
4. Record the runup point and maximum flow depth, and the time histories of flow speed and momentum flux across the entire profile as predicted by the Boussinesq simulation.
5. Using the Boussinesq predicted runup point and the onshore topographical profile, run the Energy Grade Line Analysis for a specific initial Froude number at the coastline and record maximum flow depth, flow speed, and momentum flux across the entire profile.
6. Compare the maximum flow depth, flow speed, and momentum flux predictions from the two methods.

This was implemented with a Monte Carlo simulation for randomly generated tsunami waveforms and transects, which led to the establishment of EGLA parameters that produce statistical conservatism with respect to state-of-the-art numerical solutions. The offshore profile, connecting depths of 100 to 0 m, is constructed with a single linear segment with a slope chosen randomly between $1/10$ and $1/500$, with a mean of the offshore portfolio of $\sim 1/60$. Onshore, the initial dry beach profile is composed of 20 individual linear segments with randomly chosen slope and length, where both positive and negative slope segments were allowed. A mean slope of $1/100$ for the onshore portfolio of transect cases was considered a reasonable average for all beach profiles.

The incident wave condition, as needed in Step 2, is constructed as a waveform pulse made of a single crest and trough waveform that passes through the offshore boundary of the Boussinesq-type simulation at the 100 m offshore depth. A total of 45 unique incident wave combinations were simulated for each of 800 random transect profiles, for a total of 36,000 Boussinesq-type simulations performed. On average, each transect contains roughly 20 flooded

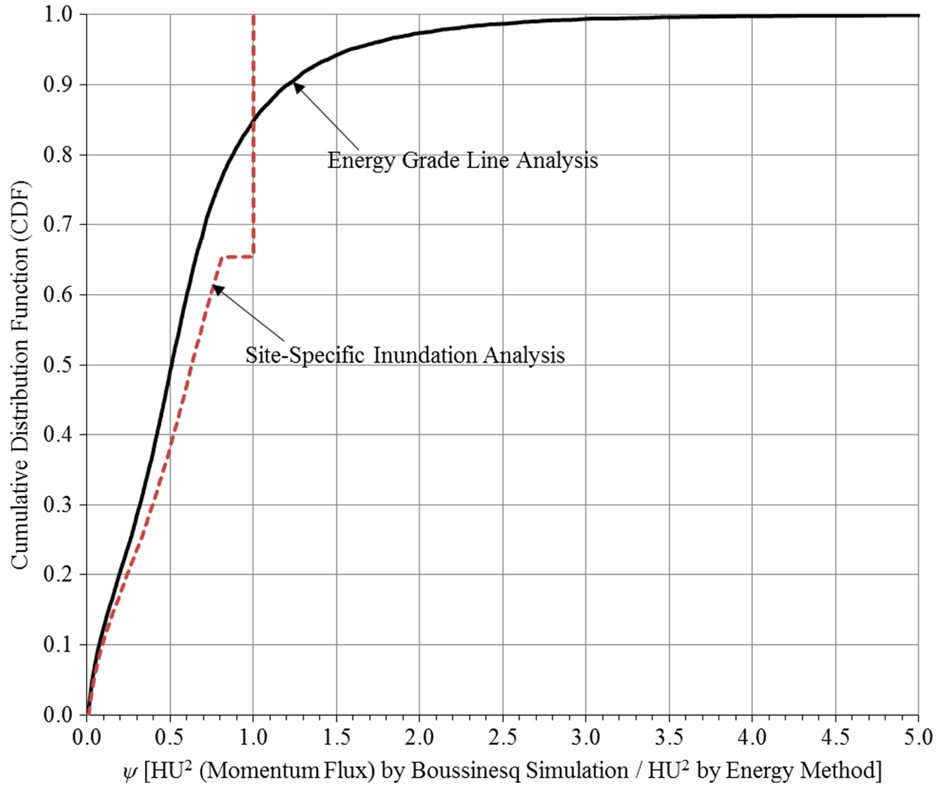

Fig. 4. Cumulative distribution functions of ψ for the prescriptive energy grade line analysis and the site-specific inundation analysis procedure

grid points, and there were over 700,000 individual point-to-point flow depth comparisons. The CDF for ψ is shown in Fig. 4. The mean and COV for ψ are 0.61 and 0.89, respectively. The EGLA was found to be generally conservative in its prediction of momentum flux, which is a desirable characteristic for design of coastal structures.

In Fig. 4, the CDF (in urban environments) fitted from the 700,000 points is also shown for the case of Tsunami Risk Category IV structures required to utilize site-specific inundation analysis subject to a minimum value set by the EGLA. The black solid curve shows that the momentum flux from the Boussinesq solution would have exceeded the EGLA for about 15% of the cases. The mean minus one standard deviation of the ELGA results are about equivalent to the mean of the Bousinnesq solution. Specifically, in urban environments, the resulting flow velocities at a given structure location shall not be reduced below 90% of those determined in accordance with the EGLA. For other terrain roughness conditions, the resulting flow velocities at a given structure location shall not be taken as less than 75% of those determined in accordance with the EGLA. The site-specific design curve of Fig. 4 includes the effect of applying the prescriptive rules for minimum design velocities to the site-specific analysis (as reflected in the discontinuities).

Tsunami Analysis and Design Parameters

The ASCE 7-16 standard classifies facilities in accordance with risk categories that recognize the importance or criticality of the facility. In the tsunami chapter, further modified definitions of the risk categories for Tsunami Risk Categories III and IV are allowed to be taken by the local government with respect to specific occupancy/functional criteria coordinated within a tsunami response plan. Critical facilities incorporates facilities needed for posttsunami mission-critical functions or facilities that have more critical roles in community recovery and community services. Critical facilities designated by local governments are included in Tsunami Risk Category III (if not already in Risk Category IV). Essential facilities are typically included in Tsunami Risk Category IV. However, certain facilities generically considered essential (such as fire stations and ambulance facilities, for example) do not need to be included in Tsunami Risk Category IV because those structures should be evacuated before the tsunami arrival, and their posttsunami functionality can then be provided from an alternate staging site.

The tsunami importance factor, I_{tsu}, is a set of assigned constants, or specified bias factors for each tsunami risk category as determined by this reliability analysis. These bias factors are included in the reliability analysis for each tsunami risk category. They were expected to be generally related to the hazard curve of overall tsunami momentum flux. Table 1 gives I_{tsu} for this reliability analysis. The tsunami parameters discussed earlier are summarized in Table 2.

The basic limit-state function $G(R,S)$ can then be parametrically given in Eq. (12):

$$G(R,S) = Z = R - S = (1/\phi)X_6X_7I_{\mathrm{TSU}} - X_1X_2X_3^2X_4^2X_5 \quad (12)$$

where R = resistance; and S = load.

Table 1. Tsunami Importance Factors for Hydrodynamic and Impact Loads

Tsunami risk category	I_{tsu}
II	1.0
III	1.25
Tsunami Risk Category IV, vertical evacuation refuges, and designated Tsunami Risk Category III critical facilities	1.25

Table 2. Reliability Analysis Parameters

Parameter	Random variable	Distribution	Mean	COV
ρ_s/ρ_{sn} (density)	X_1	Normal	1.0	0.03
C_d/C_{dn}	Constant	—	1.0	0
b/b_n (closure)—exterior column case	X_2	Uniform	0.71	0.115
h_e/h_{en} (inundation depth)	X_3	Sampled from probabilistic hazard curve		
ε (aleatory uncertainty of hazard analysis)	X_4	Lognormal	1.067	0.283
Ψ (epistemic uncertainty of flow analysis)	X_5	Sampled from the simulation curve expressing the difference between the EGLA and numerical site-specific analysis		
λ/λ_n (beam–column effect)	X_6	Lognormal	1.15	0.174
R/R_n (concrete resistance)	X_7	Normal	1.05	0.11
R/R_n (steel resistance)	X_7	Normal	1.07	0.13
I_{tsu} (tsunami importance factor)	Assigned scalar factor	In accordance with tsunami risk category (Table 1)		
ϕ (strength reduction factor)	Assigned constant	0.90 (under tsunami lateral forces and a 0.5 live-load factor, column designs become more flexurally governed)		

Reliability Analysis Using Monte Carlo Simulation

The reliabilities were calculated using Monte Carlo simulation involving a large number of trial combinations of random variables. The uncertainties of the primary variable, momentum flux is accounted for by several random variables, e.g., inundation depth, ε, and ψ. Random variable ε is modeled with a lognormal distribution and ψ is described with a summation of eight different Gaussian functions. Although an analytical Type II extreme value distribution could be well fitted to the 50-year service life maximum inundation depth of Crescent City offshore, no probability distribution could be fitted for the inland sites at Huntington Beach and Crescent City. Obviously, the distribution of load S in the limit-state equation is not normal even though a normal distribution is assumed for resistance R. So there is no closed-form solution for reliability calculation. Accordingly, Monte Carlo simulation was the most appropriate technique to employ. The procedure for the Monte Carlo simulation is as follows for the seven parameters of ρ, b, h, ε, ψ, λ, and R:

1. Randomly generate a value for each random variable in the limit-state equation. No dependence is assumed between any of the variables. The inundation depth is sampled from its 50-year service life maximum CDF curve, which is derived from the probabilistic tsunami hazard curve for the representative sites.
2. Calculate $Z = R - S$ per Eq. (12). If $G(X) = Z < 0$, then the simulated member fails.
3. Repeat Steps 1 and 2 until a predetermined number of simulations are performed.
4. Calculate the probability of failure as P_f = number of times that $Z < 0$ divided by total number of simulations.
5. The reliability index $\beta = \Phi^{-1}(1 - P_f)$.

The simulation was software-coded and generally, 1 million simulations were performed for each reliability calculation. The simulation starts at a sample size of 1 million and increased by an order of magnitude in size until convergence resulted in acceptable precision, which depended on the reliability target. For Tsunami Risk Category IV tsunami vertical evacuation refuge structures, the sample size was increased up to 250 million, since the probabilities of failure were much less than the other categories.

Results of Reliability Analysis

Tables 3 and 4 present the reliabilities and failure probabilities for representative concrete beam–column members when subject to tsunami loading (results for structural steel components would be very similar, by examining the Table 2 resistance variables).

The reliabilities were calculated with the b/b_n closure ratio design parameter for exterior columns along the building perimeter (Table 3), and without this closure ratio parameter for the case of interior columns (Table 4) that are less likely to have additional debris accumulation. The analysis of interior columns essentially ignores any incidental protective obstructions to flow within the building itself; that is, the exterior is considered as being obstructed, but the interior flow is assumed to be the same as the free-field flow. Although not evaluated in this analysis, under actual scenarios, interior columns within the building may experience lower flow speed than the exterior columns. Moreover, if debris accumulation on the exterior creates higher forces on the exterior columns, the greater solidity of the building form may also divert the flow around the structure and abate the volumetric flow rate through it. Failures of exterior columns are more commonly observed in posttsunami investigations, and so in general this is considered the more practical case of application of the reliability analysis.

The reliability indices are calculated for a 50-year service period, while the probabilities of failure have been annualized, except for the failure probabilities conditional on the occurrence of the MCT. The conditional probability of structural limit-state exceedance of a primary beam–column structural component was computed assuming the MCT has occurred, similar to the determination of the conditional reliability of the seismic provisions shown in ASCE 7's Table C.1.3.1b assuming the MCE has occurred. The conditional probabilities are thought to be a better measure of seismic design intent. For seismic and tsunami events, there is large aleatory uncertainty associated with the seismic source characterization within the probabilistic hazard analysis.

Effect of Threshold Height for Risk Category II Buildings

These tsunami reliability estimates are predicated on the assumption that the load combinations with tsunami as the primary load effect would govern the design of the members. In actual structures, the reliabilities of various members may be governed by a variety of load effects. The ASCE 7 Chapter 6, "Tsunami Loads and Effects," is recommended to apply to Risk Category II buildings greater than 19.8 m (65 ft) tall above grade plane in the most severe tsunami design zones. Such taller buildings are expected to have a robust baseline of lateral-force resistance due to seismic design requirements, and they would be seen by the public as places of refuge to get to safety above the inundation. In addition, the lower-story gravity-load-carrying columns will have a significant amount of resistance to the flexural moment of hydrodynamic

Table 3. Reliabilities for Representative Exterior Concrete Beam–Column Members

Site	Measure of reliability	Tsunami Risk Category II, I = 1.0	Tsunami Risk Category III, I = 1.25	Tsunami Risk Category IV, I = 1.25	Evacuation refuge, I = 1.25 and $1.3h_n$
Crescent City, $x = 0$	Reliability index, β	2.95	3.06	3.64	>5.75[a],
	P_{fannual}	3.2×10^{-5}	2.2×10^{-5}	2.7×10^{-6}	No failure found in
	$P_{f\text{50-year}}$ (%)	0.16	0.11	0.014	250 million trials
Crescent City, $x = 0.25x_R$	Reliability index, β	2.75	2.84	3.20	4.63
	P_{fannual}	6.0×10^{-5}	4.5×10^{-5}	1.4×10^{-5}	3.6×10^{-8}
	$P_{f\text{50-year}}$ (%)	0.30	0.22	0.07	0.00018
Crescent City, $x = 0.50x_R$	Reliability index, β	2.73	2.91	2.90	3.11
	P_{fannual}	6.3×10^{-5}	3.7×10^{-5}	3.7×10^{-5}	1.9×10^{-5}
	$P_{f\text{50-year}}$ (%)	0.31	0.18	0.19	0.09
Huntington Beach, $x = 0$	Reliability index, β	2.90	3.01	3.10	3.40
	P_{fannual}	3.7×10^{-5}	2.6×10^{-5}	1.9×10^{-5}	6.8×10^{-6}
	$P_{f\text{50-year}}$ (%)	0.19	0.13	0.097	0.034
Huntington Beach, $x = 0.25x_R$	Reliability index, β	2.78	2.87	3.11	3.79
	P_{fannual}	5.5×10^{-5}	4.1×10^{-5}	1.9×10^{-5}	1.5×10^{-6}
	$P_{f\text{50-year}}$ (%)	0.27	0.20	0.093	0.0074
Huntington Beach, $x = 0.5x_R$	Reliability index, β	2.73	2.91	2.92	3.14
	P_{fannual}	6.5×10^{-5}	3.7×10^{-5}	3.5×10^{-5}	1.7×10^{-5}
	$P_{f\text{50-year}}$ (%)	0.32	0.18	0.17	0.08
Average of the sites	Reliability index, β	**2.81**	**2.93**	**3.15**	**3.61**
	P_{fannual}	$\mathbf{5.2 \times 10^{-5}}$	$\mathbf{3.4 \times 10^{-5}}$	$\mathbf{2.1 \times 10^{-5}}$	$\mathbf{8.7 \times 10^{-6}}$
	$P_{f\text{50-year}}$ (%)	**0.26**	**0.17**	**0.11**	**0.044**
Component failure conditioned	Reliability index, β	**1.51**	**1.75**	**1.93**	**2.40**
on the occurrence of the MCT	Maximum probability of failure (%)	**6.6**	**4.0**	**2.7**	**0.82**

Note: The mean values are in boldface.
[a]This value was not included in determining the average reliability of the sites.

Table 4. Reliabilities for Representative Interior Concrete Beam–Column Members

Site	Measure of reliability	Tsunami Risk Category II, I = 1.0	Tsunami Risk Category III, I = 1.25	Tsunami Risk Category IV, I = 1.25	Evacuation refuge, I = 1.25 and $1.3h_n$
Crescent City, $x = 0$	Reliability index, β	2.80	2.91	3.08	3.33
	P_{fannual}	5.2×10^{-5}	3.7×10^{-5}	2.1×10^{-5}	8.7×10^{-6}
	$P_{f\text{50-year}}$ (%)	0.26	0.18	0.10	0.044
Crescent City, $x = 0.25x_R$	Reliability index, β	2.58	2.75	2.81	3.09
	P_{fannual}	9.9×10^{-5}	6.0×10^{-5}	4.9×10^{-5}	2.0×10^{-5}
	$P_{f\text{50-year}}$ (%)	0.4953	0.3003	0.2468	0.1011
Crescent City, $x = 0.50x_R$	Reliability index, β	2.65	2.70	2.74	2.86
	P_{fannual}	8.2×10^{-5}	7.0×10^{-5}	6.1×10^{-5}	4.3×10^{-5}
	$P_{f\text{50-year}}$ (%)	0.4093	0.3516	0.3068	0.2138
Huntington Beach, $x = 0$	Reliability index, β	2.64	2.75	2.87	3.05
	P_{fannual}	8.3×10^{-5}	6.0×10^{-5}	4.1×10^{-5}	2.3×10^{-5}
	$P_{f\text{50-year}}$ (%)	0.42	0.30	0.20	0.11
Huntington Beach, $x = 0.25x_R$	Reliability index, β	2.57	2.77	2.79	3.07
	P_{fannual}	1.0×10^{-4}	5.6×10^{-5}	5.2×10^{-5}	2.1×10^{-5}
	$P_{f\text{50-year}}$ (%)	0.5082	0.2815	0.2605	0.107
Huntington Beach, $x = 0.5x_R$	Reliability index, β	2.63	2.69	2.76	2.88
	P_{fannual}	8.6×10^{-5}	7.2×10^{-5}	5.9×10^{-5}	4.0×10^{-5}
	$P_{f\text{50-year}}$ (%)	0.431	0.361	0.2925	0.1991
Average of the sites	Reliability index, β	**2.65**	**2.76**	**2.84**	**3.05**
	P_{fannual}	$\mathbf{8.4x10^{-5}}$	$\mathbf{5.9x10^{-5}}$	$\mathbf{4.7x10^{-5}}$	$\mathbf{2.6x10^{-5}}$
	$P_{f\text{50-year}}$ (%)	**0.42**	**0.30**	**0.24**	**0.13**
Component failure conditioned	Reliability index, β	**1.14**	**1.38**	**1.45**	**1.84**
on the occurrence of the MCT	Maximum probability of failure (%)	**12.6**	**8.3**	**7.3**	**3.3**

Note: The mean values are in boldface.

pressure within each story height, just from having been designed for the $1.2D_n + 1.6L_n$ load combination for five or more floor levels. For interior columns, large debris impacts are not deemed to be a likely risk. In actual trial designs of 19.8 m (65-ft)-tall buildings (Robertson 2016), the load combination of $1.2D_n + 1.0F_{\text{TSUn}} + 0.5L_n$ for interior columns typically falls well within the axial load–moment capacity curve resulting from the element design for the $1.2D_n + 1.6L_n$ load combination. Therefore, it is concluded that the tsunami reliabilities for the interior columns are actually greater than those given just by the tsunami analysis, because the tsunami load combination is not typically the load combination governing the size of the column in multistory buildings. For

Tsunami Risk Category III and IV buildings that will have their operational functions located above the inundation depth, it is expected that minimum practical heights will be structures at least three stories tall or higher, depending on the inundation hazard at the site. For optimally designed structures, the gravity-load-carrying columns of shorter structures would tend to have somewhat less of the tsunami-resistant beneficial effect of the $1.2D_n + 1.6L_n$ load combination.

Increased Reliability with More Precise Site-Specific Inundation Analysis

The reliability analysis results in the previous section did not include the additional uncertainty in the implicit versus explicit two-dimensional evaluation of topographic amplification of flow. In the EGLA, these effects are then only implicitly considered by analysis of the given inundation limits and runup elevations within a ±22.5-degree swath about the primary design transect perpendicular to the coastline. For Tsunami Risk Category II and III structures, the prescriptive EGLA is allowed to be performed on one-dimensional topographic transects. For Tsunami Risk Category III critical facilities, Tsunami Risk Category IV structures, and tsunami vertical evacuation refuge structures, a detailed site-specific analysis is always required to be performed with detailed analysis of the two-dimensional tsunami flow depth and velocity over a high resolution (10 m or finer) digital elevation model of topography. Consequently, effects of topographic amplification of flow velocity would be explicitly determined in a site-specific inundation analysis. The tsunami design map inundation limits are produced by an inundation analysis of the two-dimensional tsunami flow depth and velocity over a medium resolution (~60 m) digital elevation model of topography. The inundation limits will accordingly express any diverting effects of the topography resulting in localized higher runups.

To evaluate the differential reliability for the Tsunami Risk Category II and III structures, the analysis is repeated with *an increase* of aleatory uncertainty sigma of 0.36 (COV of 0.34) based on the initial work by Thio et al. (2010). Tables 5 and 6 indicate the *lower* reliabilities (increased risk) that result for exterior (perimeter) and interior columns, when compared with Tables 3 and 4, respectively.

Fig. 5 summarizes the differential reliabilities as a function of the tsunami importance factors assigned to each tsunami risk category of structure, using the preceding results. For Tsunami Risk Category III critical facilities, Tsunami Risk Category IV structures, and tsunami vertical evacuation refuge structures, site-specific analysis is always required, so values of reliability for prescriptive analysis are not shown in Fig. 5. For other tsunami risk categories, site-specific analysis is permitted but not required, and therefore the minimum reliabilities (increased probabilities of exceedance) would be considered to be associated with the requirements of the ASCE 7 tsunami provisions for those categories.

Comparison with Seismic Reliabilities

The component reliabilities for the MCT rounded-off from the values of Table 3 for exterior beam–columns are compared to the systemic reliabilities given for seismic Maximum Considered Earthquake (MCE) effects (Table 7). The 50-year service life anticipated reliabilities listed in Table 7 are based on average results of the integration of the conditional (on MCE) reliabilities with seismic hazard curves from the USGS (e.g., Luco et al. 2007). The conditional probabilities (probability of failure given the occurrence of the MCE) are thought to be a better measure of seismic design intent

Table 5. Reliabilities for Representative Exterior Concrete Beam–Column Members When Site Inundation Analysis Is Performed with *Coarser* Topographic Modeling With Greater Uncertainty

Site	Measure of reliability	Tsunami Risk Category II, I = 1.0	Tsunami Risk Category III, I = 1.25
Crescent City, $x = 0$.	Reliability index, β	2.94	3.04
	$P_{fannual}$	3.3×10^{-5}	2.3×10^{-5}
	$P_{f50\text{-year}}$ (%)	0.17	0.12
Crescent City, $x = 0.25x_R$.	Reliability index, β	2.75	2.83
	$P_{fannual}$	5.9×10^{-5}	4.6×10^{-5}
	$P_{f50\text{-year}}$ (%)	0.30	0.23
Crescent City $x = 0.50x_R$	Reliability index, β	2.72	2.87
	$P_{fannual}$	6.5×10^{-5}	4.1×10^{-5}
	$P_{f50\text{-year}}$ (%)	0.32	0.20
Huntington Beach, $x = 0$	Reliability index, β	2.85	3.01
	$P_{fannual}$	4.4×10^{-5}	2.6×10^{-5}
	$P_{f50\text{-year}}$ (%)	0.22	0.13
Huntington Beach, $x = 0.25x_R$	Reliability index, β	2.78	2.86
	$P_{fannual}$	5.5×10^{-5}	4.2×10^{-5}
	$P_{f50\text{-year}}$ (%)	0.27	0.21
Huntington Beach, $x = 0.5x_R$	Reliability index, β	2.72	2.91
	$P_{fannual}$	6.6×10^{-5}	3.7×10^{-5}
	$P_{f50\text{-year}}$ (%)	0.33	0.18
Average of the sites	Reliability index, β	2.79	2.92
	$P_{fannual}$	5.4×10^{-5}	3.6×10^{-5}
	$P_{f50\text{-year}}$ (%)	0.27	0.18
Component failure conditioned on the occurrence of the MCT	Reliability index, β	1.44	1.66
	Probability of failure (%)	**7.5**	**4.9**

Note: The mean values are in boldface.

Table 6. Reliabilities for Representative Interior Concrete Beam–Column Members When Site Inundation Analysis Is Performed with *Coarser* Topographic Modeling With Greater Uncertainty

Site	Measure of reliability	Tsunami Risk Category II, I = 1.0	Tsunami Risk Category III, I = 1.25
Crescent City, $x = 0$	Reliability index, β	2.75	2.89
	$P_{fannual}$	6.0×10^{-5}	3.8×10^{-5}
	$P_{f50\text{-year}}$ (%)	0.30	0.19
Crescent City, $x = 0.25x_R$	Reliability index, β	2.57	2.74
	$P_{fannual}$	1.0×10^{-4}	6.2×10^{-5}
	$P_{f50\text{-year}}$ (%)	0.50	0.31
Crescent City, $x = 0.50x_R$	Reliability index, β	2.63	2.68
	$P_{fannual}$	8.5×10^{-5}	7.3×10^{-5}
	$P_{f50\text{-year}}$ (%)	0.43	0.37
Huntington Beach, $x = 0$	Reliability index, β	2.61	2.74
	$P_{fannual}$	9.1×10^{-5}	6.2×10^{-5}
	$P_{f50\text{-year}}$ (%)	0.46	0.31
Huntington Beach, $x = 0.25x_R$	Reliability index, β	2.57	2.74
	$P_{fannual}$	1.0×10^{-4}	6.2×10^{-5}
	$P_{f50\text{-year}}$ (%)	0.51	0.31
Huntington Beach, $x = 0.5x_R$	Reliability index, β	2.61	2.67
	$P_{fannual}$	9.0×10^{-5}	7.6×10^{-5}
	$P_{f50\text{-year}}$ (%)	0.45	0.38
Average of the sites	Reliability index, β	2.62	2.74
	$P_{fannual}$	8.8×10^{-5}	6.2×10^{-5}
	$P_{f50\text{-year}}$ (%)	0.44	0.31
Component failure conditioned on the occurrence of the MCT	Reliability index, β	1.10	1.32
	Maximum probability of failure (%)	**13.6**	**9.3**

Note: The mean values are in boldface.

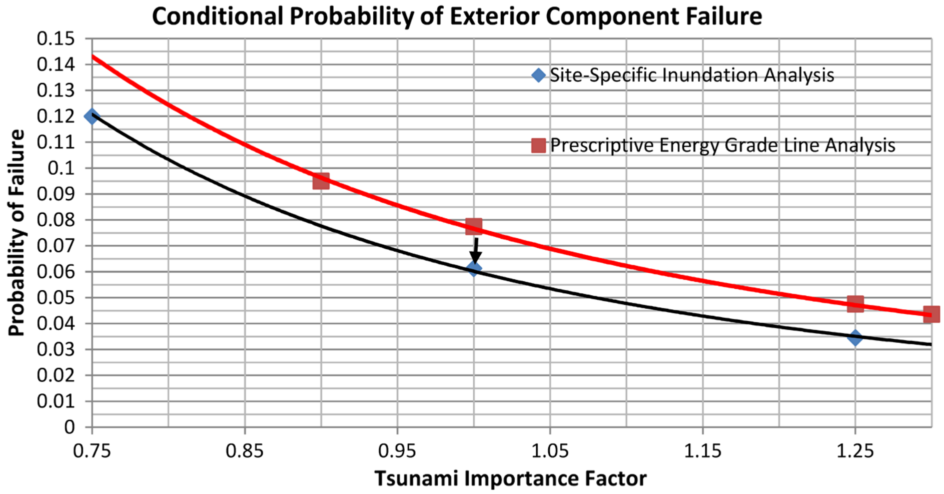

Fig. 5. Improvement in reliability due to reduction of uncertainty in analysis

Table 7. Anticipated Reliabilities (Maximum Probability of Failure) for Earthquake and Tsunami

Risk category	Probability of failure[a] in 50 years (%)		Failure[a] probability conditioned on maximum considered event (%)	
	Earthquake	Tsunami	Earthquake (MCE)	Tsunami (MCT)
II	1	0.3	10	7
III	0.5	0.2	5–6	4–5
IV	0.3	0.1	2.5–3	2.5–3
Vertical evacuation refuge structures	0.3	<0.1	2.5–3	0.5–1

[a]Tsunami probabilities are based on exceeding an exterior structural component's capacity that does not necessarily lead to widespread progression of damage, but the seismic probabilities are for the more severe occurrence of partial or total systemic collapse; probabilities for life-threatening seismic response are greater than shown in this figure; see ASCE 7-16.

within economic feasibilities; otherwise, very large additional load factors would become necessary for earthquake design to achieve the same reliabilities as the nonextraordinary cases of dead and live load design. There is no comparable structural seismic occupancy classification analogous to the tsunami vertical evacuation refuge structure, so its seismic design follows Risk Category IV.

The MCT reliabilities for Tsunami Risk Categories II and III are for the primary vertical load-carrying beam columns subjected to lateral tsunami loading, and not for the systemic (seismic) collapse mechanisms. Since in Alaska, Washington, and Oregon, the MCT is highly correlated to the occurrence of the offshore MCE in the subduction zone, it is prudent for the MCT reliabilities for the perimeter frame to be somewhat greater than for the MCE alone, especially for taller structures. Coastal structures experiencing a MCE are likely to be damaged, but most modern seismic designs are expected to retain structural integrity and then receive the MCT. Risk-targeted ground motions are defined as those which, when used to design buildings according to the ASCE standard are expected to result in buildings having a systemic collapse probability of 1% in 50 years. The 50-year service life probabilities of tsunami component failure of the exterior elements along the building perimeter are less than the 1, 0.5, and 0.3% systemic collapse probability in 50 years for Risk Category II, III, and IV structures, respectively, that are the basis of the present-day risk-targeted maximum considered earthquake ground motion maps and seismic importance factors (Luco et al. 2007). The tsunami probabilities are consistent with the occurrence of potentially life-endangering structural component response, but the seismic probabilities are for the more severe occurrence of partial or total systemic collapse.

The risk-targeted maximum considered earthquake response (MCER) probabilistic analysis includes the accounting of epistemic uncertainties of the seismic source characterization through logic trees and structural system performance through fragility functions, and some aleatory uncertainty in characteristic moment magnitude (assumed to be distributed within ± 0.15; the seismic maps do not have explicit accounting for aleatory uncertainty at the seismic source other than the magnitude) and in the ground motion prediction (i.e., use of a standard deviation bias in the empirical attenuation equations). Therefore, there could be greater uncertainty in the seismic systemic reliabilities given in Table 7.

Component Reliability versus System Reliability

There is an inherently strong bias in the design strength of the lateral-load-resisting system due to seismic requirements and the minimum height of the structure. Studies of steel and concrete structures have identified the beneficial effect of the seismic design requirements for the lateral-force-resisting system capacity to resist tsunami loads (Chock et al. 2013). For example, the structural height of 19.8 m (65 ft) recommended for general applicability of the tsunami provisions for Tsunami Risk Category II buildings in the Pacific Northwest provides this margin [Figs. 6(a and b)] against inundation depths of about 12.2 m (40 ft). In this figure of a prototypical example, the solid line represents the system inelastic capacities for each height of building. The dashed curves represent the hydrodynamic loading as inundation increases during the tsunami. Hydrodynamic drag assumes the buildings are 30% open (Chock et al. 2013). For these cases, it was assumed that the overall shear on the lateral-load-resisting system governed rather than building overturning. Seismically designed masonry structures should be similar to the RC structures in this consideration. The structural steel moment frame is assumed to have member sizes just sufficient to meet drift limitations. Due to flexibility that affects the natural period and prescribed loads, the total base shear capacity does not increase sharply with midrise height increases. This would imply that a material weight-optimized steel moment frame system

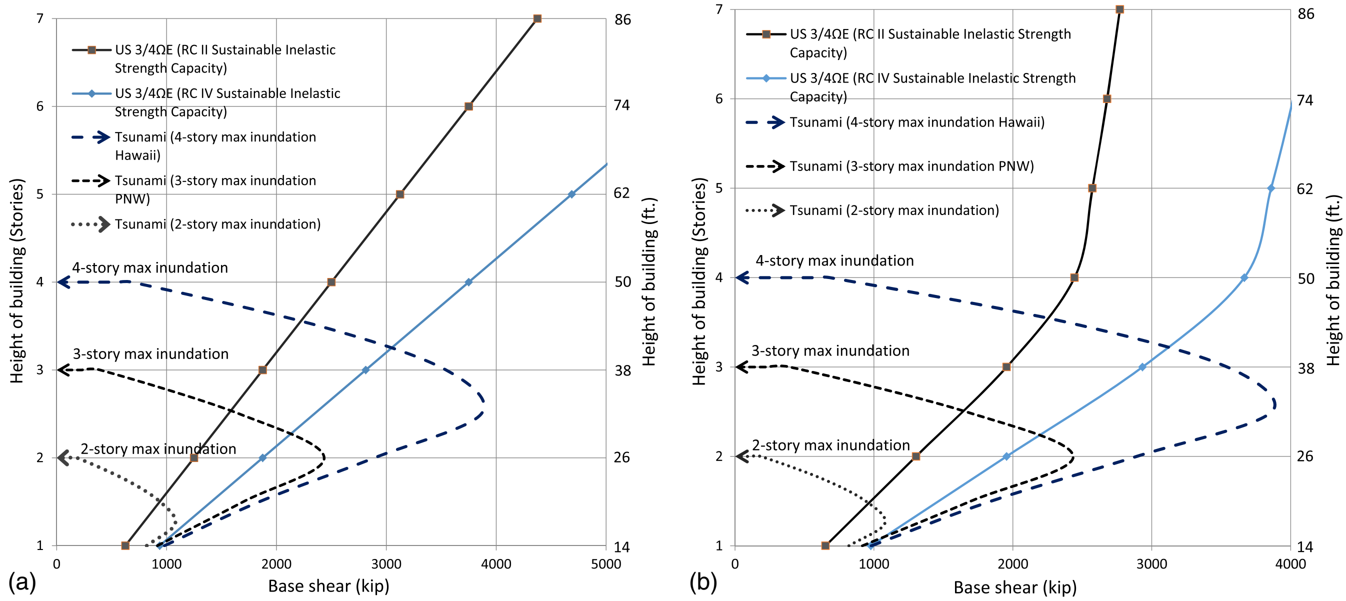

Fig. 6. (a) Comparisons of seismic base shear capacity and overall tsunami shear force for concrete structural walls, with increasing building height and tsunami depth on the vertical axis; (b) comparisons of seismic base shear capacity and overall tsunami shear force for steel moment-resisting frames designed for maximum permissible seismic drift, with increasing building height and tsunami depth on the vertical axis

may need some increased capacity beyond the prescriptive minimum seismic demand, if located in a site with severe inundation depths greater than about 40 ft.

Midrise to high-rise buildings, which are necessary for tsunami safety where evacuation cannot be completely assured, can be economically designed for life safety or better performance for large tsunamis with local strengthening of relatively few components. To do similar comparisons for Tsunami Risk Category III and IV structures, the comparison would also include accounting for the seismic importance factor increase of seismic capacity, which would shift the capacity curves to the right by factors of 1.25 and 1.50, respectively, and provide more of a margin against tsunami forces. Accordingly, Risk Category III and IV structures will have a lower threshold height of structural parity between the systemic strength for lateral forces acquired through the seismic provisions and the resistance necessary for sustained tsunami lateral forces.

Conclusions

The values of tsunami importance factors have been analytically determined from the target structural reliabilities, which were calculated using Monte Carlo simulation involving a large number of trial combinations of random variables independently occurring in proportion to their statistical distributions for the demand parameters of fluid density, closure ratio, energy grade line momentum flux, inundation depth hazard, and the aleatory uncertainty of inundation depth. Reliability analysis was performed for both exterior and interior gravity-load-carrying vertical beam–columns subject to lateral tsunami loading. Failures of exterior columns are more commonly observed in posttsunami investigations, and this is considered the more practical case of application of the reliability analysis for the reasons discussed in this paper. Target structural component reliabilities given in case the maximum considered tsunami (MCT) has occurred are similar to seismic systemic performance reliabilities given in case the maximum considered earthquake (MCE) has occurred. These reliability estimates are predicated on the assumption that the load combinations with tsunami as the primary load effect would govern the design of the members. In actual structures, the reliabilities of various members may be governed by a variety of load effects. In ASCE 7-16, it is stated that structural components designed with performance-based procedures shall be demonstrated using an analysis to provide a reliability not less than the target reliabilities. Therefore, the recommended tsunami target structural reliability values are given in the last row of Table 8, for use in performance-based engineering of structural components designed to meet the intent of ASCE 7-16, Chapter 6 ("Tsunami Loads and Effects").

For Tsunami Risk Category II, a tsunami importance factor of 1.0 results in a structural component limit-state capacity conditional exceedance probability of approximately 7.5% (MCT).

Table 8. Summary of Target Reliabilities of the ASCE 7 Tsunami Design Provisions

Basis	Measure of reliability	Tsunami Risk Category II, I = 1.0	Tsunami Risk Category III, I = 1.25	Tsunami Risk Category IV, I = 1.25	Tsunami vertical evacuation refuge RC IV, I = 1.25 and $1.3h_n$
Average reliabilities	Reliability index, β	2.74	2.87	3.03	3.68
	$P_{f50\text{-year}}$ (%)	0.31	0.21	0.13	0.05
Component failure conditioned on the occurrence of the MCT	Reliability index, β	1.44	1.65	1.92	2.43
	Probability of component failure (%)	**7.5**	**5**	**3**	< **1**

Note: The mean values are in boldface.

ASCE 7 gives a conditional failure probability of 10% (MCE) for collapse of the lateral-force-resisting system during an earthquake.

For Tsunami Risk Category III, a tsunami importance factor of 1.25 results in a structural component limit-state capacity conditional exceedance probability of approximately 5% (MCT). ASCE 7 gives a conditional failure probability of 5–6% (MCE) for collapse of the lateral-force-resisting system during an earthquake.

For Tsunami Risk Category IV, a tsunami importance factor of 1.25 and site-specific inundation analysis results in a structural component limit-state capacity conditional exceedance probability of approximately 3% (MCT). ASCE 7 gives a conditional failure probability of 2.5–3% (MCE) for collapse of the lateral-force-resisting system during an earthquake.

For tsunami vertical evacuation refuge structures, the tsunami importance factor of 1.25 and site-specific inundation analysis, combined with the prescriptive requirement to use a 1.3 factor on the site-specific inundation depth, results in a structural component limit-state capacity conditional exceedance probability of less than 1% (MCT). ASCE 7 gives a conditional failure probability of 2.5–3% (MCE) for collapse of the lateral-force-resisting system of Risk Category IV structures during an earthquake.

This analysis indicates that the new ASCE 7 tsunami design provisions will result in a design with a level of reliability for structural components generally equivalent to or exceeding the targeted reliabilities for other types of extraordinary loadings such as maximum considered earthquake events.

Acknowledgments

The support of the American Society of Civil Engineers, Structural Engineering Institute, and the Coasts, Oceans, Ports, and Rivers Institute, towards the development of the tsunami design provisions in ASCE 7-16 by the Tsunami Loads and Effects Subcommittee is gratefully acknowledged.

References

ASCE/SEI (Structural Engineering Institute). (2016). “Minimum design loads for buildings and other structures.” *ASCE/SEI 7-16*, Reston, VA.

California Geological Survey. (2015). “Evaluation and application of probabilistic tsunami hazard analysis in California.” *Special Rep. 237*, Sacramento, CA.

Carden, L., Chock, G., Yu, G., and Robertson, I. N. (2015). “The new ASCE tsunami design standard applied to mitigate Tohoku tsunami building structural failure mechanisms.” *Handbook of coastal disaster mitigation for engineers and planners*, M. Esteban, H. Takagi, and T. Shibayama, eds., Butterworth-Heinemann (Elsevier), Waltham, MA.

Chock, G. (2015). “The ASCE 7 tsunami loads and effects design standard for the U.S.” *Handbook of coastal disaster mitigation for engineers and planners*, M. Esteban, H. Takagi, and T. Shibayama, eds., Butterworth-Heinemann (Elsevier), Waltham, MA.

Chock, G. (2016). “Design for tsunami loads and effects in the ASCE 7-16 standard.” *J. Struct. Eng.*, in press.

Chock, G., Carden, L., Robertson, I., Olsen, M., and Yu, G. (2013). “Tohoku tsunami-induced building failure analysis with implications for U.S. tsunami and seismic design codes.” *Earthquake Spectra*, 29(S1), S99–S126.

Ellingwood, B. (1977). “Statistical analysis of RC beam-column interaction.” *J. Struct. Div.*, 103(ST7), 1377–1388.

Ellingwood, B., Galambos, T. V., MacGregor, J. G., and Cornell, C. A. (1980). “Development of a probability based load criterion for American national standard A58.” National Bureau of Standards, Washington, DC.

Luco, N., Ellingwood, B. R., Hamburger, R. O., Hooper, J. D., Kimball, J. K., and Kircher, C. A. (2007). “Risk-targeted versus current seismic design maps for the conterminous United States.” *Structural Engineers Association of California Annual Conf. Proc.*, Structural Engineers Association of California, Sacramento, CA, 163–175.

Lynett, P., and Liu, P. (2011). “Numerical simulation of complex tsunami behavior.” *Comput. Sci. Eng.*, 13(4), 50–57.

Robertson, I. N. (2016). “Tsunami loads and effects: Guide to the tsunami design provisions of ASCE 7-16.” ASCE, Reston, VA.

Thio, H. K., Somerville, P., and Polet, J. (2010). “Probabilistic tsunami hazard in California, Pacific earthquake engineering research center.” *PEER Rep. 2010/108*, Univ. of California, Berkeley, CA.